

Energy Management and Control of Distributed Generation Inverter in a Domestic Smart Grid Technology



M. Shameem

PG Scholar,
Dept of EEE (EPS),
Srinivasa Institute of Technology
& Sciences, Kadapa,
Andhra Pradesh, India.



Seetha Chaithanya

Assistant Professor,
Dept of EEE,
Srinivasa Institute of Technology
& Sciences, Kadapa,
Andhra Pradesh, India.



G. Venkata Suresh Babu

Associate Professor & HOD,
Dept of EEE,
Srinivasa Institute of Technology
& Sciences, Kadapa,
Andhra Pradesh, India.

Abstract:

Microgrids are a new concept for future energy distribution systems which enable renewable energy integration and improved energy management capability. They can be intended as back-up power or to bolster the main power grid during periods of heavy demand. Even microgrids entail many energy sources as a way of incorporating renewable power. Microgrid consisting of multiple Distributed Generator (DG) units connected to the distribution grid is presented in this project. To enhance power quality and also to enhance the reliability of power distribution and it need to operate in both grid-connected and island modes. The different distributed generator units are photovoltaic (PV) array which functions as the primary generation unit of the microgrid and a proton-exchange membrane fuel cell to supplement the variability in the power generated by the PV array.

The key factor of using DGs lies on how to coordinate DGs with main grid to stable and reliable running and for this an energy-management algorithm is implemented. A storage battery not only helps in reducing peak demands but also compensates any shortage of generated power during grid connected and islanded operation respectively. The control design for the DG inverters employs a new model predictive control algorithm which enables faster computational time for large power systems by optimizing the steady-state and the transient control problems separately. The performance is verified via simulation results.

Key words:

Distributed generation (DG), Energy Management, microgrid, Model Predictive Control(MPC).

I.INTRODUCTION:

Microgrid is a new concept which plays a very important role in the future distribution network system. This project gives a centralized control nothing but coordinated control and energy management between the distributed generation inverters in a micro grid under various operating conditions like grid connected mode and islanded mode. Grid connected mode means the distribution grid is coupled with the considered micro grid and the islanded mode means the distribution grid is disconnected with the micro grid under such condition there is a mutual control between the distributed generation inverters in order to meet the particular demand. Renewable energy generations such as wind, solar panels, PV systems, fuel cells and storage devices may act as distributed generations where the proposed system consisting of a PV array, proton exchange membrane fuel cell (PEMFC), and a lithium-ion storage battery (SB) these all connected to the distribution grid.

These three renewable energy generations act as distribution generation units in the micro grid. The DG units interfaced with the power electronic inverters called as distributed generation inverters. To control these DG inverters we employed a new concept called model predictive control (MPC). This MPC control reduces the computational time very greatly by analyzing both the steady state as well as transient problems separately. The PV array and the PEMFC both are acting as the main DG unit in which the PEMFC act as a backup generator unit if there is any problem in the PV array because of its intermittent nature. The lithium-ion storage battery in the microgrid is implemented for both peak shaving and islanded condition, in the grid connected operation it mitigates

the peak demands and in the islanded operation it act to compensate for any shortage in the generated power. Energy storage elements such as storage batteries and some capacitors called ultra capacitors needed to compensate for the variations in the renewable generations where PV array and the proton exchange membrane fuel cell. In the microgrid generally there are problems divided into steady state as well as transient problems these are studied separately and optimally by the MPC controller to reduce the time required for its computation.

If the controller other than MPC gives more computational time which is not desired in the microgrid conditions, like PI, PD, PID controllers they reduce the steady state error and improves the damping of the system they need more time for analyzing the problems. There is a concept of demand side management and demand response management is also involved in this project there is a energy management algorithm is designed for the microgrid to coordinate the dispatching of power between different distribution generation units.

II. SYSTEM DESCRIPTION AND MODELING:

A. System Description:

Fig. 1 shows the configuration of the microgrid proposed in this paper that is designed to operate either in the grid-connected or islanded mode. The main DG unit comprises a 40-kW PV array and a 15-kW PEMFC, which are connected in parallel to the dc side of the DG inverter 1 through dc/dc boost converters to regulate the dc-link voltage of the DG inverter at the desired level by delivering the necessary power. The PV array is implemented as the primary generation unit and the PEMFC is used to back up the intermittent generation of the PV array. When there is ample sunlight, the PV array operates in the MPPT mode to deliver maximum dc power P_{pv} , and the output voltage of the PV array is permitted to vary within an allowable range to ensure proper operation of the DG inverter. balance in the microgrid which is given by

$$P_{DG} + P_b = P_L \tag{1}$$

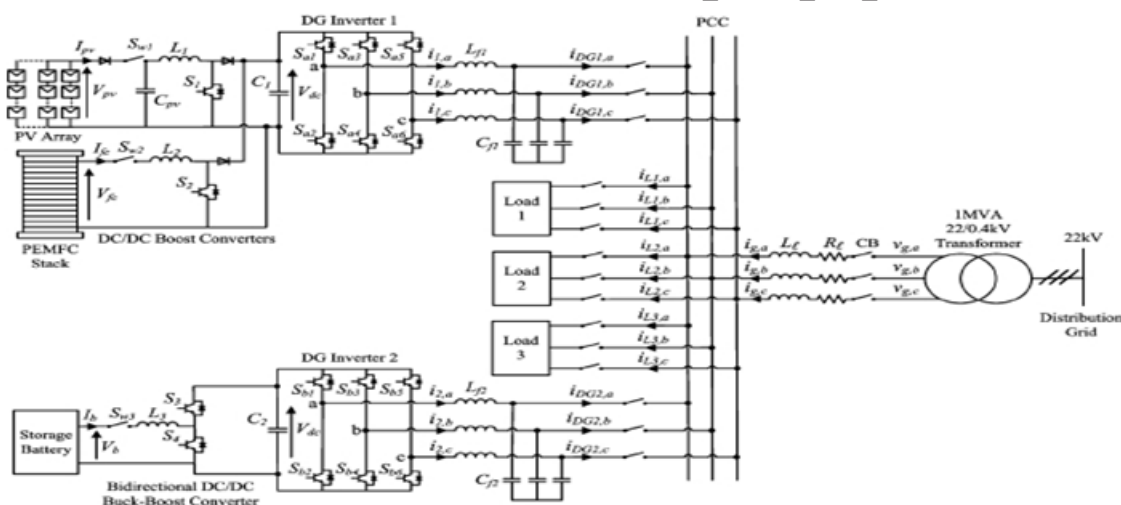


Fig.1. Overall configuration of the proposed microgrid architecture

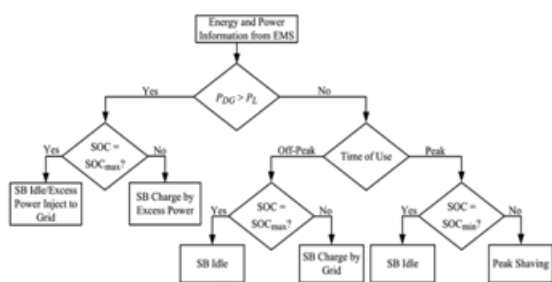
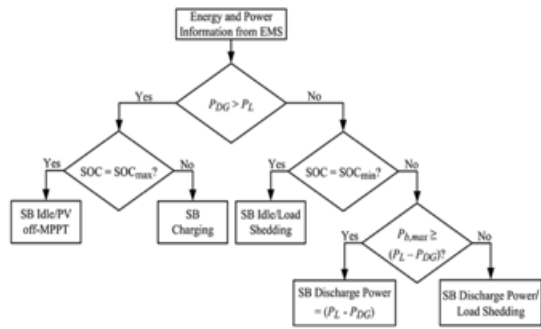


Fig.2. Operation of the SB during grid connection operation.

To maintain the level of the dc-link voltage V_{dc} at the required level, the PEMFC supplements the generation of the PV array to deliver the necessary P_{fc} . When the output voltage of the PV array falls below a preset limit, the PV array is disconnected from the DG unit and the PEMFC functions as the main generation unit to deliver the required power. A 30-Ah lithium-ion SB is connected to the dc side of DG inverter 2 through a bidirectional dc/dc buck-boost converter to facilitate the charging and discharging operations. During islanded operation, the role of the SB is to maintain the power



Where P_{DG} is the power delivered by the main DG unit, P_b is the SB power which is subjected to the charging and discharging constraints given by

$$P_b \leq P_{b,max} \quad (2)$$

and P_L is the real power delivered to the loads. The energy constraints of the SB are determined based on the state-of-charge (SOC) limits which are given as

$$SOC_{min} < SOC \leq SOC_{max} \quad (3)$$

During grid-connected operation, the distribution grid is connected to the micro grid at the point of common

coupling(PCC) through a circuit breaker(CB). The role of the main DG unit functions to provide local power and voltage support for the loads and, hence, reduces the burden of generation and delivery of power directly from the distributed grid. With the proliferation of power-electronics equipment being connected to the microgrid, the load currents could be distorted due to the presence of harmonic components. When the total load demand exceeds the generation capacity of the main DG unit and the SB, the EMS detects a drop in the system frequency and load shedding for noncritical loads is required to restore the system frequency and maintain the stability of the microgrid.

B. DG Inverter Modeling:

Figs. 4 and 5 show the equivalent single-phase representation of the DG inverters for grid-connected and islanded operation, respectively [13]–[15]. The switched voltage across the output of the j th DG inverter is represented by $u_j V_{dcj}$, where u_j is the control input and $j = 1, 2$. The output of the DG inverter is interfaced with an LC filter represented by L_{fj} and C_{fj} to eliminate the high switching frequency harmonics generated by the DG inverter. The resistance R_j models the loss of the DG inverter. The total load current i_L , which is the sum of the currents delivered to the load k ($k = 1, 2, 3$), is given by

$$i_L = \sum_{k=1,2,3} i_{Lk} = i_{L1} + i_{L2} + i_{L3} \quad (4)$$

and can be modeled as two components consisting of fundamental i_{Lf} and harmonic i_{Lh} with their peak amplitudes I_{Lf} and I_{Lh} , respectively, and is represented by

$$\begin{aligned} i_L &= i_{Lf} + i_{Lh} = I_{Lf} \sin(\omega t - \varphi_{Lf}) \\ &+ \sum_{h=3,5,\dots}^N I_{Lh} \sin(h\omega t - \varphi_{Lh}) \\ &= I_{Lf} \sin \omega t \cos \varphi_{Lf} - I_{Lf} \cos \omega t \sin \varphi_{Lf} \\ &+ \sum_{h=3,5,\dots}^N I_{Lh} \sin(h\omega t - \varphi_{Lh}) \\ &= i_{Lf,p} + i_{Lf,q} + i_{Lh} \end{aligned} \quad (5)$$

where φ_{Lf} and φ_{Lh} are the respective phase angles of the fundamental and harmonic components of i_L , and $i_{Lf,p}$ and $i_{Lf,q}$ are the instantaneous fundamental phase and quadrature components of i_L . To achieve unity power factor at the grid side, compensate for the harmonics in the load currents and concurrently achieve load sharing, the inverter of the DG unit supplies a current i_{DGj} that is given by

$$i_{DGj} = (i_{Lf,p} - i_g) + i_{Lf,q} + i_{Lh} \quad (6)$$

where i_g is the grid current. As shown in Fig. 4, the distribution grid is supplied by a utility substation represented by a voltage source v_g during grid-connected operation, and is connected to the microgrid and the loads via a distribution line with resistance R_l and inductance L_l .

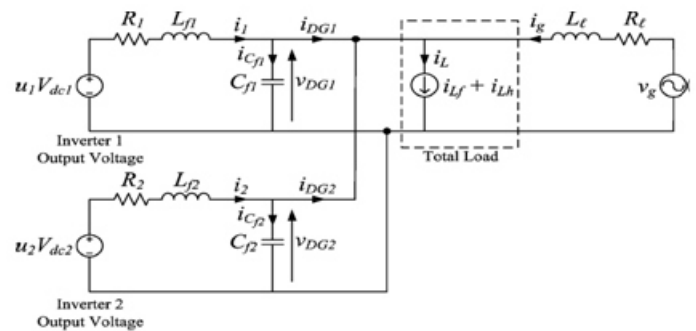


Fig.4. Equivalent single-phase representation of the DG inverters for grid connected operation.

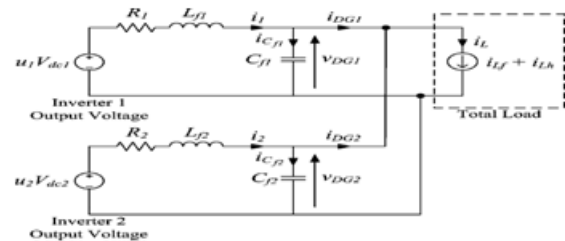


Fig.5. Equivalent single-phase representation of the DG inverters for islanded operation.

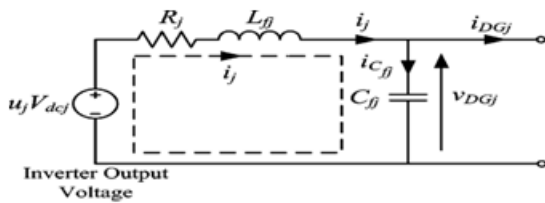


Fig.6 single-phase representation of the *j*th DG inverter for grid-connected and islanded operations.

To derive a state-space model for the DG inverter during both grid-connected and islanded operations, Kirchhoff's voltage and current laws are applied to the current loop i_j as shown in Fig. 6, and the following equations are obtained:

$$\frac{di_j}{dt} = -\frac{R_j}{L_{fj}} i_j - \frac{1}{L_{fj}} v_{DGj} + \frac{V_{dcj}}{L_{fj}} u_j \quad (7)$$

$$\frac{dv_{DGj}}{dt} = \frac{1}{C_{fj}} i_j - \frac{1}{C_{fj}} i_{DGj} \quad (8)$$

where i_j is the current passing through L_{fj} . Hence the grid-connected DG inverter model can be written as

$$x_{gj} = A_{gj} x_{gj} + B_{gj1} v'_j + B_{gj2} u_j \quad (9)$$

$$y_{gj} = C_{gj} x_{gj} + D_{gj1} v_j + D_{gj2} u_j \quad (10)$$

Where the subscripts *g* and *j* represent the model of DG inverter *j* during grid-connected operation ($j=1, 2$) and

$$A_{gj} = -\frac{R_j}{L_{fj}} ; B_{gj1} = \left[\frac{1}{L_{fj}} \quad 0 \right] ; B_{gj2} = \frac{V_{dcj}}{L_{fj}}$$

$$C_{gj} = 1 ; D_{gj1} = [0 \quad -C_{fj}] ; D_{gj2} = 0$$

$x_{ij} = i_j$ is the state; $v'_j = [v_{DGj} \quad dv_{DGj}/dt]^T$ is the exogenous input; u_j is the control input, with $-1 \leq u_j \leq 1$; and $y_{gj} = i_{DGj}$ is the output, which will be regulated to track the desired periodic reference waveform.

During islanded operation, the frequency will change due to power imbalance in the microgrid. This change in frequency is detected by the EMS of the microgrid, which is used to manage and monitor the power dispatch by each DG unit. Based on the frequency change information, the EMS will require the main DG unit and the SB to generate the necessary power to meet the overall load demand in the microgrid as shown in the flowchart of Fig. 3, such that (1) is satisfied. During islanded operation, it follows from (7) and (8) that DG inverter *j* can be modeled as

$$x_{ij} = A_{ij} x_{ij} + B_{ij1} i'_j + B_{ij2} u_j \quad (11)$$

$$y_{ij} = C_{ij} x_{ij} + D_{ij1} i_j + D_{ij2} u_j \quad (12)$$

Where the subscript *i* denotes the model of the DG inverter *j* during islanded operation ($j = 1, 2$) and

$$A_{ij} = \begin{bmatrix} -\frac{R_j}{L_{fj}} & -\frac{1}{L_{fj}} \\ \frac{1}{C_{fj}} & 0 \end{bmatrix} ; B_{ij1} = \begin{bmatrix} 0 \\ -\frac{1}{C_{fj}} \end{bmatrix} ; B_{ij2} = \begin{bmatrix} \frac{V_{dcj}}{L_{fj}} \\ 0 \end{bmatrix}$$

$$C_{ij} = \begin{bmatrix} 0 & 1 \\ 1 - \frac{C_{fj}}{C'_f} & 0 \end{bmatrix} ; D_{ij1} = \begin{bmatrix} 0 \\ \frac{C_{fj}}{C'_f} \end{bmatrix} ; D_{ij2} = \begin{bmatrix} 0 \\ 0 \end{bmatrix}$$

with $C'_f = \sum_{j=1}^2 C_{fj}$; $x_{ij} = [i_j \quad v_{DGj}]^T$ is the state vector ;

$i'_j = i_L - \sum_{n \neq j} i_n$ is the exogenous input of the DG inverter *j*; u_j is the control input, with $-1 \leq u_j \leq 1$; and $y_{ij} = [v_{DGj} \quad i_{DGj}]^T$ is the output, which will be regulated to track the desired reference waveform. Note that although the emphasis is on the voltage v_{DGj} , both v_{DGj} and i_{DGj} will be regulated in the VCM to ensure that the power is delivered. Furthermore, it is assumed that the exogenous input i'_j in the model is not directly measurable by the DG inverter *j* since it involves quantities outside that inverter. Precisely, i'_j represents the sum of all load currents i_L minus the sum of all i_n from the other DG inverters $n \neq j$ in the microgrid. Although only one other inverter has been presented in the proposed microgrid, the model is extendable to more DG inverters.

III. CONTROL DESIGN:

With the mathematical model presented in section II-B, this paper proposes a novel MPC algorithm for the control of the DG inverters of the microgrid. The proposed algorithm is a newly developed MPC algorithm specifically designed for fast-sampling systems, to track periodic signals so as to deal with the dual-mode operation of the microgrid. The algorithm decomposes the MPC optimization into a steady-state sub-problem and a transient sub-problem, which can be solved in parallel in a receding horizon fashion.

Furthermore, the steady-state sub-problem adopts a dynamic policy approach in which the computational complexity is adjustable. The decomposition also allows the steady-state sub-problem to be solved at a lower rate than the transient sub-problem if necessary. These features help to achieve a lower computational complexity and make it suitable for implementation in a fast-sampling system like our microgrid applications.

In the simulation studies in this paper, the sampling interval is chosen as 0.2ms, which is considered pretty small in conventional MPC applications, but necessary for the high order of harmonics being tackled for our problem. According to [16], sampling in the range of tens of kHz is possible with state-of-the-art code generation techniques. It is noted that in either the grid-connected or the islanded operation, the state-space model of Section II-B after time-discretization will take the form

$$x^+ = Ax + B_1\omega + B_2u \quad (13)$$

$$y = Cx + D_1\omega + D_2u \quad (14)$$

where the superscript + represents the time-shift operator (with sampling interval T_s), and the exogenous signal is periodic. In general, any periodic signal with a finite number of harmonics can be written as the output of an autonomous finite-dimensional linear time-invariant state-space model. For example, if the periodic signal has a fundamental frequency and consists of only odd harmonics, the A-matrix of the corresponding state-space model can take a block diagonal

form with the blocks given by $\begin{bmatrix} \cos(h\omega T_s) & \sin(h\omega T_s) \\ -\sin(h\omega T_s) & \cos(h\omega T_s) \end{bmatrix}$

where $h = 1, 3, 5, \dots$ and the C-matrix $[1 \ 0 \ 1 \ 0 \ \dots \ 1 \ 0]$. Furthermore, the initial state of this autonomous model determines the magnitude and phase angle of this periodic signal. Hence, the exogenous signal ω in (13) and (14) together with the reference d that y in (14) desires to track can be modeled by

$$\xi^+ = A_\xi \xi \quad (15)$$

$$\omega = C_\omega \xi \quad (16)$$

$$d = C_d \xi \quad (17)$$

for some A_ξ , C_ω and C_d as described above. For the CCM during grid-connected operation, $y = i_{DG}$ and the current reference $d = di_{DG}$ for i_{DG} to track consist of the same order of harmonics as i_L and is derived from the desired active and reactive power outputs of the DG units generated by the EMS.

The state-space model given by (15)-(17) is known as the exogenous system in this paper. Although only odd harmonics up to the 29th order have been considered, the methodology can be easily extended to include even harmonics. The exogenous state ξ , which essentially represents the sets of Fourier coefficients of ω and d , can be automatically identified using a Kalman-based observer known as the exogenous Kalman filter once the signal ω is measured and the reference d is specified. The exogenous Kalman filter is given by

$$\xi^+ = A_\xi \xi + L_\omega(\omega - \tilde{\omega}) + L_d(d - \tilde{d}) \quad (18)$$

$$\tilde{\omega} = C_\omega \xi \quad (19)$$

$$\tilde{d} = C_d \xi \quad (20)$$

where ξ is the estimated exogenous state, L_ω and L_d are the observer gain matrices of the Kalman filter, and the terms $(\omega - \tilde{\omega})$ and $(d - \tilde{d})$ are essentially the difference between the actual ω and d and the estimated $\tilde{\omega}$, \tilde{d} generated from the Kalman filter, such that $(\omega - \tilde{\omega})$ and $(d - \tilde{d})$ should tend to zero asymptotically. Since ξ is actually a Fourier decomposition of the periodic signals ω and d , the exogenous Kalman filter given by (18)–(20) functions like a harmonic extraction circuit from the power system point of view [17], [18].

In what follows, the control u in (13) and (14) is decomposed into a steady-state control u_s and a transient control u_t as

$$u = u_s + u_t \quad (21)$$

Such that $u \rightarrow u_s$ and $u_t \rightarrow 0$ asymptotically. Both u_s and u_t will employ a MPC strategy, but the former will adopt a dynamic MPC policy whereas the latter will adopt a more conventional finite-horizon approach.

A.Simulink Diagram:

The simulation model is designed for the proposed microgrid system by using MATLAB software is shown in fig.7

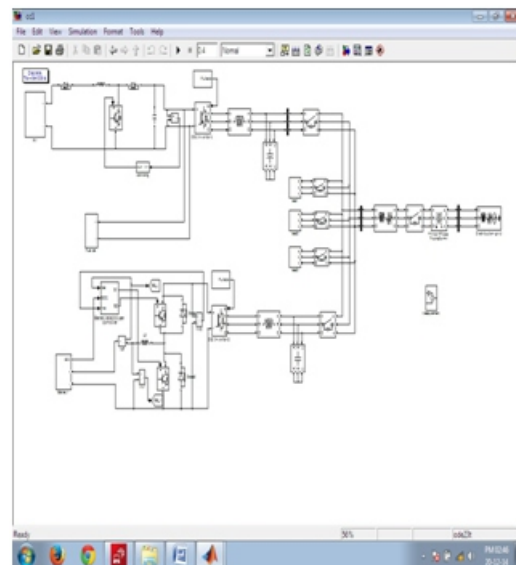


Fig.7. Simulink model for the proposed microgrid system

The simulink model consisting of the blocks of PV array, fuel cell and the storage battery which are the main renewable energy resources in the proposed system.the

microgrid is tested under various conditions to evaluate its capabilities when operating connected and islanded from the distribution grid.

B. Power quality improvement with load sharing during grid connected operation:

Power quality improvement with load sharing during grid connected operation demonstrates the capacity of the microgrid to improve the power quality of the distribution network by compensating the harmonics in the total load current due to the nonlinear loads that are connected to the distribution network, such that the harmonics will not propagate to the rest of the distribution network during grid connected operation. The SB current for $0 \leq t < 0.4$ are shown in fig.8.1. The SB is operating in the charging mode to store energy during off-peak period where the cost of generation from the grid is low to meet future sudden demands for power.



Fig.8.1. Waveform of the SB current during charging

The waveform of the total load current for $0 \leq t < 0.4$ is shown in fig.8.2.

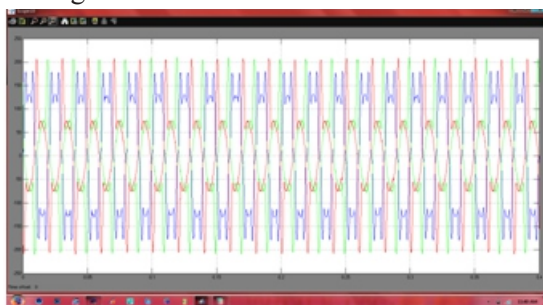


Fig.8.2. Waveform of three phase load current

There is no unsteady measurements in the waveform of the three phase load current but in the waveforms of three phase DG current and three phase grid current the unsteady measurements are present for $0 \leq t < 0.06$. The total real power and reactive power delivered to the loads is about 58kW and 35kVAR. The real power delivered to the load is shown in fig.8.3

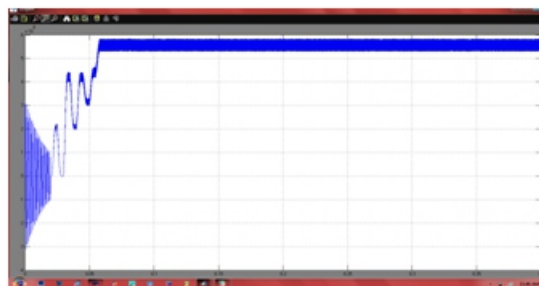


Fig.8.3. Real power consumed by loads

The real power is nothing but the useful power consumed by the loads but the reactive power consumed by the load is also considered to get the apparent power. The reactive power consumed by the loads is shown in fig.8.4.

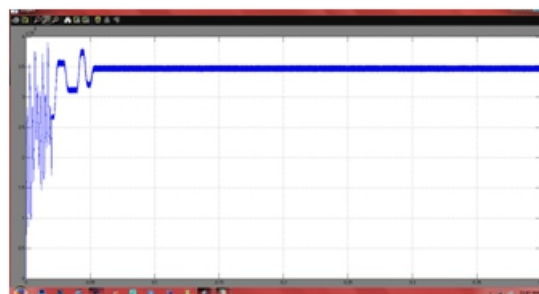


Fig.8.4. Reactive power consumed by loads

The real power dispatched by the main DG unit is 20% of the real power consumed by the loads. The real power delivered by the main DG unit is shown in fig.8.5

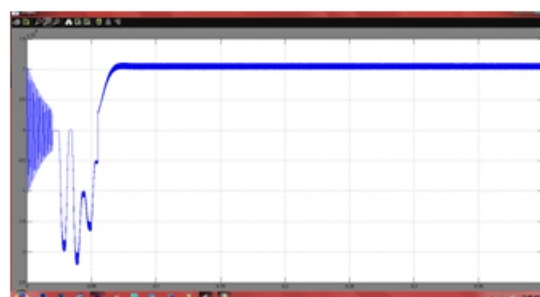


Fig.8.5. Real power delivered by the main DG unit

C. Peak shaving of loads during peak periods:

Peak shaving of loads during peak periods demonstrates the operation of the microgrid to achieve peak shaving in order to reduce the cost of generation from the distribution grid.

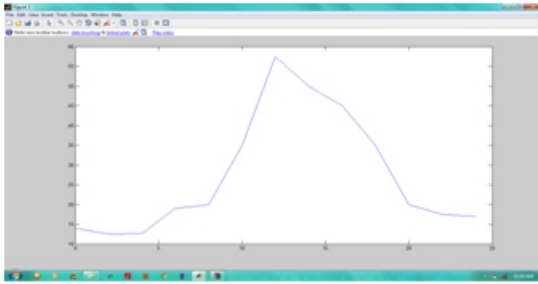


Fig.9. Hourly demand response curve

The fig.9 shows a typical hourly demand response curve in which the demand is varying. The real power delivered by the grid is 60% of the load demand with peak shaving. to achieve peak shaving at 11:00 h the SB is operating in the discharge mode to provide 20% of the load demand.

D. Load shedding during islanded operation:

During islanded operation the total generation of the microgrid not be able to sustain its generation to meet the power demand of the loads.

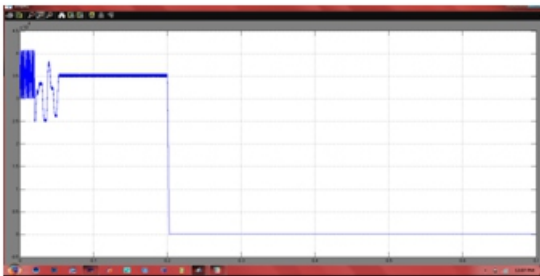


Fig.10.1. Real power delivered by the grid

The real power delivered by the grid is shown in fig.10.1 The microgrid is initially in the grid connected mode for $0 \leq t < 0.2$ s. the SB is initially operating in the idle mode. A fault occurs on the upstream network of the distribution grid and the CB operates to disconnect the microgrid from the distribution grid at $t=0.2$ s. Up to $t=0.2$ s the SB is in idle mode after that the real power delivered by the SB is shown in fig.10.2.

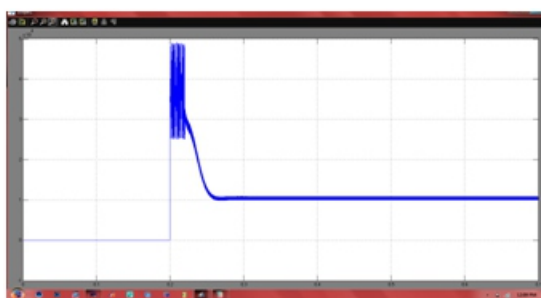


Fig.10.2. Real power delivered by the SB

The real power delivered to the loads for $0 \leq t < 0.6$ s is shown in fig.10.3 Generally when load 3 is shed at $t=0.4$ s. the total real and reactive power delivered to the loads gradually decreases.



Fig.10.3. Real power consumed by the loads

The reactive power delivered to the loads for $0 \leq t < 0.6$ s is shown in fig.10.4



Fig.10.4. Reactive power consumed by the loads

when load 3 is shed the total real and reactive power delivered to the loads gradually decreases settle and operate stably at about 40kW and 22.7 kVAr respectively.

V. CONCLUSION:

This project proposed a control and management strategy for optimal and reliable operation of a microgrid for grid connected and islanded operations. The strategy uses Photovoltaic array (PV) as main power supply and DGs, storage battery as slave power supply. Coordination between multiple DGs in a microgrid system can be realized by using control system. MPC algorithm is implemented in the proposed controller which decomposes the control problem into steady-state and transient sub problems in order to reduce the overall computation time. The results have validated that the microgrid is able to handle different operating conditions effectively during grid-connected and islanded operations, thus increasing the overall reliability and stability of the microgrid.

REFERENCES:

- [1] S. Braithwait, "Behaviormangement," IEEE Power and EnergyMag., vol. 8, no. 3, pp. 36-45, May/Jun. 2010.
- [2] N. Jenkins, J. Ekanayake, and G. Strbac, Distributed Generation. London, U.K.: IET, 2009.
- [3] M. Y. Zhai, "Transmission characteristics of low-voltage distribution networks in China under the smart grids environment," IEEE Trans. Power Del., vol. 26, no. 1, pp. 173–180, Jan. 2011.
- [4] G. C. Heffner, C. A. Goldman, and M. M. Moezzi, "Innovative approaches to verifying demand response of water heater load control," IEEE Trans. Power Del., vol. 21, no. 1, pp. 1538–1551, Jan. 2006.
- [5] R. Lasseter, J. Eto, B. Schenkman, J. Stevens, H. Vollkommer, D. Klapp, E. Linton, H. Hurtado, and J. Roy, "Certs microgrid laboratory test bed, and smart loads," IEEE Trans. Power Del., vol. 26, no. 1, pp. 325–332, Jan. 2011.
- [6] A. Molderink, V. Bakker, M. G. C. Bosman, J. L. Hurink, and G. J. M. Smit, "Management and control of domestic smart grid technology," IEEE Trans. Smart Grid, vol. 1, no. 2, pp. 109–119, Sep. 2010.
- [7] A. Mohsenian-Rad, V. W. S.Wong, J. Jatskevich, R. Schober, and A. Leon-Garcia, "Autonomous demand-side management based on gametheoretic energy consumption scheduling for the future smart grid," IEEE Trans. Smart Grid, vol. 1, no. 3, pp. 320–331, Dec. 2010.
- [8] S. Chowdhury, S. P. Chowdhury, and P. Crossley, Microgrids and Active Distribution Networks. London, U.K.: IET, 2009.
- [9] A. Yazdani and P. P. Dash, "A control methodology and characterization of dynamics for a photovoltaic (PV) system interfaced with a distribution network," IEEE Trans. Power Del., vol. 24, no. 3, pp. 1538–1551, Jul. 2009.
- [10] K. T. Tan, P. L. So, Y. C. Chu, and K. H. Kwan, "Modeling, control and simulation of a photovoltaic power system for grid-connected and stand-alone applications," in Proc. Int. Power Energy Conf., 2010, vol. 56, pp. 608–613.

Author's Profile:

M.Shameem, has received the B.Tech (Electrical and Electronics Engineering) degree from Global College of Engineering and Technology, Kadapa in 2012 and pursuing M.Tech (Electrical Power Systems) in Srinivasa institute of Technology & Sciences, Kadapa, AP, India.

Seetha chaithanya, has 5 years of experience in teaching in both Graduate and Post Graduate level and he is presently working as Assistant Professor in department of EEE in SITS, Kadapa, AP, India.

G. Venkata Suresh Babu, has 13 years experience in teaching in both Graduate and Post Graduate level and he is presently working as Associate Professor and HOD of EEE department in SITS, Kadapa, AP, India.